

Modern Physics Letters B
© World Scientific Publishing Company

Dirty Bosons: Twenty Years Later

Peter B. Weichman

*BAE Systems, Advanced Information Technologies,
6 New England Executive Park, Burlington, MA 01803, USA
peter.weichman@baesystems.com*

Received (Day Month Year)

Revised (Day Month Year)

A concise, somewhat personal, review of the problem of superfluidity and quantum criticality in regular and disordered interacting Bose systems is given, concentrating on general features and important symmetries that are exhibited in different parts of the phase diagram, and that govern the different possible types of critical behavior. A number of exact results for various insulating phase boundaries, which may be used to constrain the results of numerical simulations, can be derived using large rare region type arguments. The nature of the insulator-superfluid transition is explored through general scaling arguments, exact model calculations in one dimension, numerical results in two dimensions, and approximate renormalization group results in higher dimensions. Experiments on ^4He adsorbed in porous Vycor glass, on thin film superconductors, and magnetically trapped atomic vapors in a periodic optical potential, are used to illustrate many of the concepts.

Keywords: Boson superfluidity; disordered systems; quantum phase transitions.

1. Introduction

It has been approximately 20 years now since the flowering of interest in the dirty boson problem. The problem is defined, generally, as the nature of the insulating and conducting phases, and the phase transitions between them, in a system of interacting bosons in a random potential at zero temperature. A phase transition occurring at zero temperature, as a function of some auxiliary control parameter, such as density or magnetic field, is known as a *quantum phase transition* (QPT) since the particle dynamics are provided purely by the fluctuations in the ground state wavefunction.^a In a Bose system the conducting phase is believed always to be a superfluid (SF) (see, e.g., Ref. 4), and this strongly distinguishes the dirty boson

^aAt finite temperature, through standard arguments (see, e.g., Ref. 1) quantum mechanics is irrelevant near criticality, and the physics reduces to that of the corresponding classical model—the XY-model in the case of superfluid ^4He . The effects of disorder are then governed by the well known Harris criterion (Ref. 2). For discussion specific to bosons on a disordered substrate, and further references, see Ref. 3.

2 *Peter B. Weichman*

problem from the corresponding Anderson localization and metal-insulator transition problems in Fermi systems.^{5,6} In particular, the conducting phase has a natural order parameter, absent in an ordinary metal, associated with the off-diagonal long range order of the superfluid. Moreover, in the absence of Pauli exclusion, repulsive interactions are essential in forestalling condensation of a macroscopic number of particles into the single lowest localized free particle eigenstate of the random potential. There is therefore no sensible noninteracting limit about which to perturb to study the physical finite density phases. Thus, although there are some analogies between the Fermi and Bose phenomena, the underlying physics is very different, and the two problems require entirely different theoretical approaches to their solution.

1.1. *Some “ancient” history*

Perhaps the earliest relevant experiments, which certainly were key to motivating early work on the dirty boson problem,⁷ were on superfluidity of very thin films of ⁴He adsorbed in porous Vycor glass.⁸ Vycor glass has a highly connected, 40% open (well above the percolation threshold), 3D sponge-like structure with pore sizes in the 4–8 nm range. In an interesting historical reversal, the experiments themselves were motivated not by disorder effects, but by the claimed earliest experimental evidence for an essentially ideal Bose gas, a dozen years in advance of its observation in magnetically trapped atomic vapors!^{9,10} Of course, the Vycor system is not nearly as “clean” as the atomic system (in senses that should become clear below), so the claim itself is not as clean as might be desired.^b

Some of the Vycor superfluid density (ρ_s) vs. temperature data⁸ are reproduced in the upper left panel of Fig. 1. The ideal Bose glass claim emerged from an examination of the evolution of the shapes of the $\rho_s(T; \rho)$ profiles in the vicinity of the transition $T_c(\rho)$ as the overall helium density ρ was reduced. It was observed⁸ that the exponent ν describing the superfluid onset power law, $\rho_s \sim |t|^\nu$ below T_c , where $t = (T - T_c)/T_c$ is the reduced temperature, showed a clear crossover from the classic bulk value, $\nu \simeq 2/3$, observed at higher coverages, toward the ideal Bose gas value, $\nu_0 = 1$, at the lowest coverages. Quantitative theoretical predictions for this crossover, based entirely on a clean, non-disordered “effective medium” model,^{11,12,13} were generally consistent with this scenario.

Although the trends in the vicinity of T_c support an ideal gas interpretation, other elements of the data definitely do not, and this will serve as motivation for the remainder of this article. Motivated by QPT ideas, the remaining panels of Fig. 1 show plots involving various zero temperature quantities.¹³ In the upper right panel is plotted the extrapolated zero temperature superfluid density $\rho_s(0; \rho)$ vs. ρ (the horizontal axis should be divided by the 0.89 cm³ total glass-plus-pore volume

^bThe essential role of Vycor is that it acts to screen the long-range attractive part of the helium-helium pair potential, which in the bulk causes the vapor to condense into a dense fluid, preempting observation of the dilute regime in pure, bulk ⁴He.

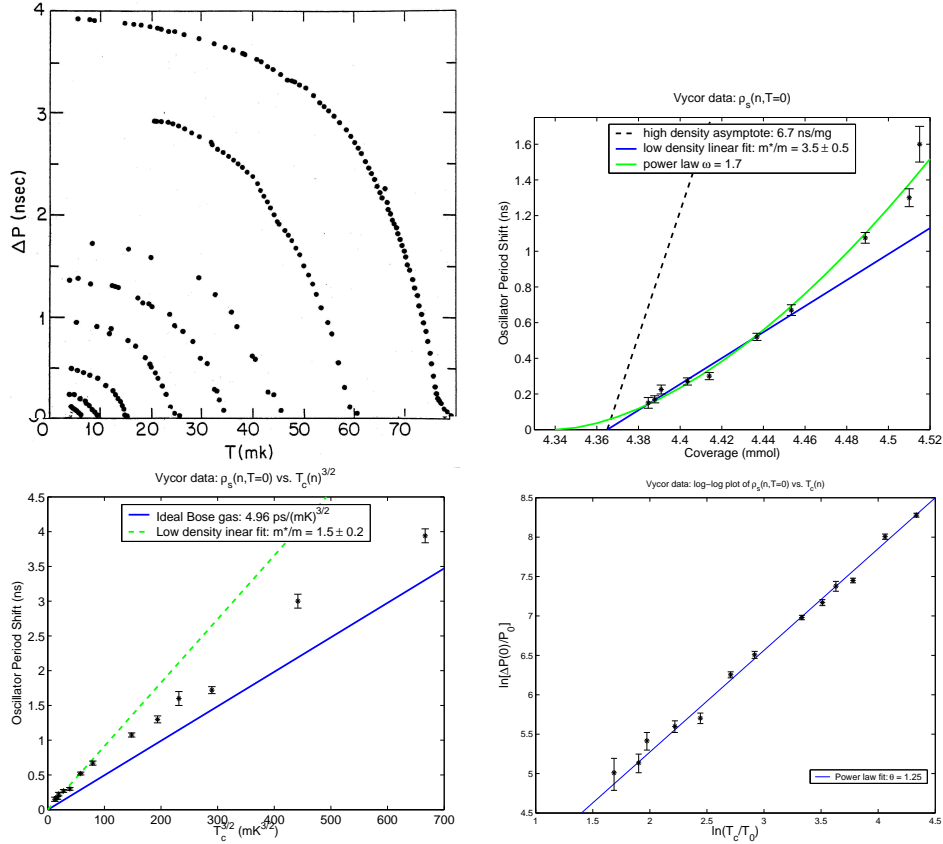


Fig. 1. Superfluidity of helium in Vycor. **Upper left:** Superfluid density (proportional to the torsional oscillator period shift ΔP due to the decoupling of the superfluid from the oscillating substrate) data for ^4He adsorbed in porous Vycor glass. The different curves correspond to different fixed values of the overall filling. The trend with decreasing coverage ρ , towards a more linear, less steep, onset just below the transition temperature $T_c(\rho)$, is evident to the eye. **Upper right:** Extrapolated zero temperature superfluid density vs. coverage, with fits to ideal Bose gas and QPT-motivated functional forms. **Lower left:** Extrapolated zero temperature superfluid density vs. T_c compared to ideal gas models. **Lower right:** QPT-motivated power-law fit to the zero temperature superfluid density vs. T_c data.

if one is fussy about units). Zero temperature superfluidity evidently disappears for $\rho < \rho_c \simeq 4.35$ mmol, corresponding to a coverage of about 1.5 monolayers (over the estimated 156 m^2 pore surface area). If one interprets ρ_c to be an inert background upon which the superfluid component “floats,” then an ideal gas model would predict a linear relation $\rho_s(0; \rho) \propto \rho - \rho_c$. Evidently, one may force a linear fit to the lowest density data by adjusting the slope using an effective mass free parameter. The fitted value $m^*/m \simeq 3.5$ is at least consistent with one’s intuition that interaction with the substrate would tend to increase the mass. However,

a more convincing fit, over a much wider range, is obtained with a superlinear fit $\rho_s(0; \rho) \propto (\rho - \rho_c)^\omega$, which serves to define our first QPT critical exponent $\omega \simeq 1.7 \pm 0.3$.

The bottom two panels of Fig. 1 compare the rates at which $\rho_s(0; \rho)$ and $T_c(\rho)$ vanish with ρ . An ideal gas model predicts $T_c \propto \rho^{d/2}$, with spatial dimensionality $d = 3$ here. The lower left panel shows that one may force such a proportionality over the lower coverage data, again using an effective mass free parameter. The fact that the inferred value $m^*/m \simeq 1.5$ is *different* from the previous one should lead to some discomfort. Once again, as seen in the log-log plot of the same data in the right panel, a much more satisfactory power-law fit $\rho_s(0; \rho) \propto T_c(\rho)^\theta$ is obtained, with a second QPT critical exponent $\theta = 1.25 \pm 0.2$.^c

1.2. Outline

With the helium in Vycor system serving as an introduction, the outline of the remainder of this paper is as follows. This review is not intended to be comprehensive, and the author apologizes in advance for his personal choices as to which developments deserve emphasis. In Sec. 2 the theoretical approach to the problem is introduced through the Bose-Hubbard and Josephson junction lattice models. In Sec. 3, the phases, phase diagrams, and accompanying phase transitions are motivated and summarized. In Sec. 4, exact results for the incompressible phase boundaries, based on the existence of exponentially rare, but arbitrarily large, disorder free regions, are derived. In Sec. 5 the quantum model is mapped onto a classical field theory Lagrangian. The various parameters appearing in the latter allow one to transparently identify the different possible symmetries of the model, and accompanying QPT universality classes. In Sec. 6, QPT critical scaling phenomenology is introduced, which, in particular, allows one to express the exponents ω and θ in terms of more familiar ones. Scaling also predicts the existence of universal sheet conductances in $d = 2$, which has some experimental support. Renormalization group and epsilon expansion approaches to detailed model calculations are discussed in Sec. 7. The latter are poorly controlled compared to their classical counterparts, but nevertheless provide an compelling global picture of the stability, bifurcation, and merging of critical fixed points as a function of dimension that is consistent with the phenomenological scaling arguments. The review is summarized and concluded

^cWhy, over a large range of coverages, is the behavior near T_c consistent with an ideal Bose gas crossover, while over the same range the zero temperature quantities show strong deviations? The answer is not entirely clear but, firstly, critical scaling near T_c is entirely separate from QPT scaling near $T = 0$ —for a detailed discussion of this in the context of the clean system, see Ref. 14. Thus, disorder is expected to have distinctly different impacts on the two ends of the superfluid density profile. Second, as discussed in Ref. 3, its manufacturing process makes Vycor very uniform on multi-pore scales, which aids the uniform effective medium approximation which forms the basis of the ideal gas model. However, one eventually expects to see strong deviations, as the disorder begins to impact the ideal Bose gas physics, presumably at yet smaller values of $\rho - \rho_c$ that are beyond experimental resolution.

in Sec. 8.

2. Bose-Hubbard and Josephson junction Models

In analogy to the Hubbard model of electronic propagation in a crystalline solid, a useful starting point for the study of bosons in a disordered medium is the Bose-Hubbard model of lattice bosons. The Hamiltonian is

$$\mathcal{H}_B = -J \sum_{\langle i,j \rangle} \hat{a}_i^\dagger (\hat{a}_j - \hat{a}_i) - \mu \sum_i \hat{n}_i + \frac{1}{2} V \sum_i \hat{n}_i (\hat{n}_i - 1) + \sum_i u_i \hat{n}_i, \quad (1)$$

in which $\hat{a}_i^\dagger, \hat{a}_i$ are boson creation and annihilation operators on site i (taken to lie on a regular lattice, and obeying the usual Bose commutation relations $[\hat{a}_i, \hat{a}_j^\dagger] = \delta_{ij}$), $\hat{n}_i = \hat{a}_i^\dagger \hat{a}_i$ is the (non-negative integer) site number operator, the first sum is over nearest neighbors, $J = \hbar^2/2m^*d^2$ is the hopping amplitude, where d is a measure of the pore diameter and m^* is a boson effective mass, μ is the chemical potential, $V > 0$ the on-site repulsion, and u_i the random site energies. In this model each site represents a pore, and the microscopic structure of the individual pores has been subsumed into the model effective parameters. The same picture obtains for bosons hopping between minima of the optical lattice potentials that are used to perturb magnetically trapped atomic vapors.^{15,16} Clearly, a more realistic model would include disorder in J , V , and the lattice site positions, but, as in the fermion case, these add nothing new to the basic physics implied by the random u_i . One could also add higher order Hubbard bands, corresponding to higher order intra-pore single particle excited states, but at low temperatures, lacking Pauli exclusion, these will not be populated, and can be ignored. The precise probability distribution of the u_i is not important, but it is useful to consider them as independent from site to site, with an even distribution (in particular, with mean zero, which normalizes the chemical potential), and with support on a finite interval $-\Delta \leq u_i \leq \Delta$, with the bound Δ serving as a free parameter.

A closely related model is the Josephson junction, or quantum rotor model,

$$\mathcal{H}_J = - \sum_{\langle i,j \rangle} J_{ij} \cos(\hat{\phi}_i - \hat{\phi}_j) - \mu \sum_i \hat{n}_i + \frac{1}{2} V \sum_i \hat{n}_i^2 + \sum_i u_i \hat{n}_i, \quad (2)$$

in which $\hat{n}_i, \hat{\phi}_i$ are conjugate number and phase operators, defined by the commutation relations $[\hat{\phi}_i, \hat{n}_j] = i\delta_{ij}$. In this model \hat{n}_i can take negative as well as positive integer values. The mapping between the two models is provided by identifying $\hat{a}_i^\dagger \leftrightarrow \hat{n}_i^{1/2} e^{i\hat{\phi}_i}$, $\hat{a}_i \leftrightarrow e^{-i\hat{\phi}_i} \hat{n}_i^{1/2}$. This Hamiltonian originated as a model of granular superconductors, with \hat{n}_i representing the number of Cooper pairs on grain i , and with Josephson couplings J_{ij} between the phases of the neighboring grains. The hopping term clearly lowers the energy when neighboring phases are aligned, and the superfluid, or superconducting, state corresponds to the appearance of long range order, and corresponding nonzero local averages $\langle e^{i\hat{\phi}_i} \rangle \neq 0$ [corresponding to the usual Bose condensate $\langle \hat{a}_i \rangle \neq 0$ in (1)]. Quantitative agreement between the

two models is obtained in the limit of large mean site occupancy $n_i = \langle \hat{n}_i \rangle \gg 1$, where number fluctuations can be neglected in the hopping term and one identifies $J_{ij} \approx J\sqrt{n_i n_j}$.

By separating amplitude and phase in this way the underlying symmetries of the model, which are critical to identifying the possible QPT universality classes, are much more transparently exhibited. First note that under an integer translation $\hat{n}_i \rightarrow \hat{n}_i + n_0$, which preserves the commutation relations, the Hamiltonian transforms in the form,

$$\mathcal{H}_J(\mu) \rightarrow \mathcal{H}_J(\mu - n_0 V) + \left(-\mu n_0 + \frac{1}{2} V n_0^2\right) N_L, \quad (3)$$

where N_L is the number of lattice sites. It follows that the phase diagram is periodic in μ with period V (see Fig. 4; the additive constant serves simply to increase the overall density by n_0). Second, the particle-hole transformation corresponds to the reflections,

$$\hat{n}_i \rightarrow -\hat{n}_i, \quad \hat{\phi}_i \rightarrow -\hat{\phi}_i, \quad (4)$$

which also preserves the commutation relations. Under this transformation, $\mathcal{H}(\mu, \{u_i\}) \rightarrow \mathcal{H}(-\mu, \{-u_i\})$. Together with the translation symmetry, this implies that at the special values $\mu = n_0 V/2$, in the absence of site disorder, $u_i \equiv 0$ (but arbitrary J_{ij}), the Hamiltonian is invariant (up to an additive constant), implying the existence of a special symmetry between particle and hole excitations. Furthermore, for symmetrically distributed u_i , the transformed Hamiltonian is *statistically* identical to the original. In either case, the phase diagram has an additional reflection symmetry about the points $\mu = n_0 V/2$.

These special *particle-hole symmetric* and *statistically particle-hole symmetric* points (which \mathcal{H}_B can only exhibit indirectly—see below) will play an important role in understanding the critical behavior. Furthermore, the fact that the hopping is unaffected by the transformation motivates consideration of disorder in both $J_{ij} = J(1 + \delta J_{ij})$ (which serves to define an overall control parameter J) and u_i in this model. Understanding the effects of breaking these symmetries (which ultimately leads back to \mathcal{H}_B , but now understood in a broader context) will turn out to be key to understanding the global renormalization group flows (Sec. 7).

3. Phases and phase diagrams

By considering the energy balance between the various terms in (1) and (2) one can understand the basic topology of the phase diagrams. First the results for the Bose-Hubbard model (1) will be motivated and presented. Additional features special to the Josephson junction model (2) will then be discussed. Detailed calculations can be found in the literature: the original mean field predictions for the phase diagram were made in Ref. 7; subsequent perturbation calculations can be found in Ref. 23, 24, and numerical simulations can be found, for example, in Refs. 17, 18, 19, 20, 21, 22.

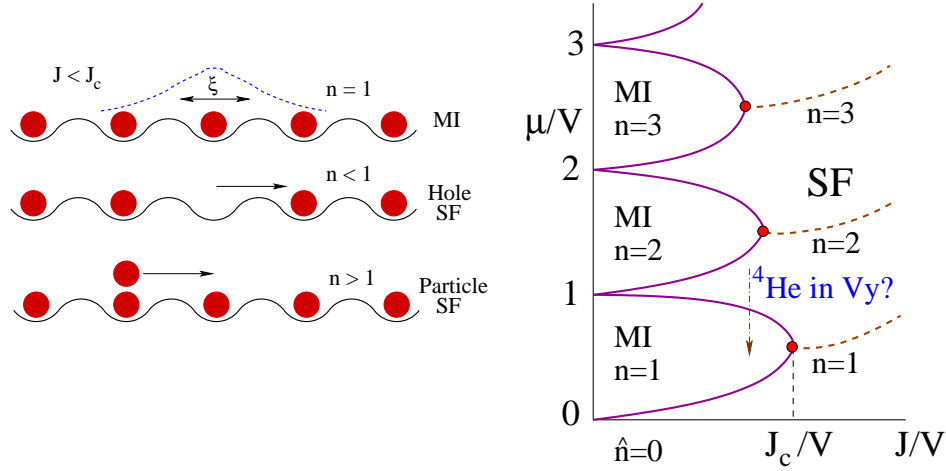


Fig. 2. **Left:** Schematic illustration of lattice bosons near unit filling $n = 1$ at some value of the hopping amplitude in the interval $0 < J < J_c$. In the Mott insulating phase ($n = 1$), the effective wavefunction of each particle spreads only a finite distance $\xi(J)$, and the state is insulating. For $n > 1$ ($n < 1$), the extra particles (holes) travel freely within the essentially inert background, and the state is superfluid for arbitrarily small $|n - 1|$. **Right:** Associated phase diagram with Mott insulating (MI) and superfluid (SF) phases. The MI are incompressible, with fixed integer filling over a finite range of μ . The SF is compressible, with integer filling only along some set of lines extending from the Mott lobe tips. The phase transition through the tip, where a “hidden” particle-hole symmetry is asymptotically restored, is in the universality class of the $(d + 1)$ -dimensional classical XY model. Elsewhere, the transition is equivalent to onset of superfluidity at zero density in a continuum dilute Bose gas. In this sense, as indicated, “periodic Vycor” would indeed produce the desired ideal Bose gas crossover upon approach to integer filling.

3.1. Clean system

We begin with the clean, non-disordered system, $u_i \equiv 0$, corresponding to bosons moving in a perfectly periodic background potential. The left panel of Fig. 2 sketches the essential physics. If there is no hopping, $J = 0$, then the sites decouple, the site occupancies are good quantum numbers, and there are exactly n_0 particles on each site for $n_0 < \mu/V < n_0 + 1$. There is a unit jump in filling at each integer value of μ/V . For finite J , particles are no longer confined to a single site, but may wander to neighboring sites. However, for small J/V the mutual repulsion produces an energy gap of order V whenever two particles occupy the same site. So, although virtual exchanges do occur, the net effective distance $\xi(J, n_0)$ a given particle wanders remains finite. There is a corresponding energy gap $\mu_{\pm}(J, n_0) = \pm[E(J, n_0 N_L \pm 1) - E(J, n_0 N_L)]$, where $E(J, N)$ is the ground state energy for N particles, for adding (+) or removing (−) a particle. Thus, for chemical potential in the interval $\mu_{-}(J, n_0) < \mu < \mu_{+}(J, n_0)$, the ground state wavefunction is insensitive to μ , and, in particular, the density remains fixed at n_0 . This incompressible phase is known as a Mott insulator (MI), analogous to the corresponding electron half-filled band insulators, and the resulting lobe structure of the phase diagram is

sketched in right panel of Fig. 2. All of these notions can be confirmed through direct perturbation theory in J/V .^{23,24}

Only for sufficiently large J is the hopping sufficiently vigorous to overcome the repulsion: at a critical value $J \rightarrow J_c(n_0)$ the hopping range diverges, $\xi \rightarrow \infty$, and the gap closes, $\varepsilon_{\pm} \rightarrow 0$. For $J > J_c$ one enters the superfluid phase. One may define a quantum critical exponent correlation length exponent ν via $\xi \sim |J - J_c|^{-\nu}$, and dynamical exponent z via $\varepsilon_{\pm} \sim |J - J_c|^{z\nu}$. It will be shown in Sec. 5 that this transition, at which, as alluded to above, an *effective* particle-hole symmetry is restored, is in the universality class of the classical $(d+1)$ -dimensional XY model: $\nu = \nu_{d+1}^{\text{XY}}$, $z = 1$. Thus, for example, in $d = 2$, $\nu_3^{\text{XY}} \simeq 0.671$ should be the same as that measured at the ^4He lambda transition.

Between Mott lobes, $\mu_+(J, n_0) < \mu < \mu_-(J, n_0 + 1)$, the density varies continuously between the two integer values, $n_0 < n(\mu, J) < n_0 + 1$. Near the Mott lobe boundaries one may think of the difference $n - n_0$ as extra particles (or $n_0 + 1 - n$ as extra holes) propagating atop the Mott phase background. Now lacking a barrier to hopping between sites, these particles (or holes) form a superfluid (lower left part of Fig. 2). Although the notion of coexisting insulating and superfluid components is misleading (bosons are identical particles, and there is strong exchange between the two groups), the effective theory near the phase boundary (analogous, perhaps, to the Fermi liquid theory of effectively free electron excitations near the Fermi surface) is indeed that of a dilute Bose gas. The exchange with the background insulator gives rise to a strongly renormalized (especially near J_c) effective single particle mass m^* . In this sense, if Vycor had perfectly periodic pores, experiments would indeed see a crossover to dilute Bose gas behavior, with $\rho_c = n_0/d^3$ corresponding to the density at integer filling. Perhaps the closest experimental realization is that of trapped atomic vapors in an additional imposed optical lattice.^{15,16} However, although both MI and SF phases have been detected in these experiments, trap inhomogeneities, finite size effects, and other measurement constraints, are such that detailed critical phenomena are not yet resolvable.

As stated, the very different critical behaviors at the “commensurate” transition at J_c , and the line of “incommensurate” transitions below J_c are indicative of a “hidden” particle-hole symmetry at the former. The lack of an exact symmetry in \mathcal{H}_B means that this symmetry is effectively restored at the nontrivial point where $\mu_+(J_c, n_0) = \mu_-(J_c, n_0)$ (analogous to the asymptotic restoration of the underlying Ising up-down symmetry of density fluctuations near a liquid-vapor critical point). During the transition to superfluidity at integer filling, particle and hole excitations exist in equal numbers, tunneling through each other, and achieve superfluidity simultaneously. Below J_c the transition takes place by feeding extra particles or holes into the system, explicitly breaking this symmetry, and only the predominant excitation achieves superfluidity.

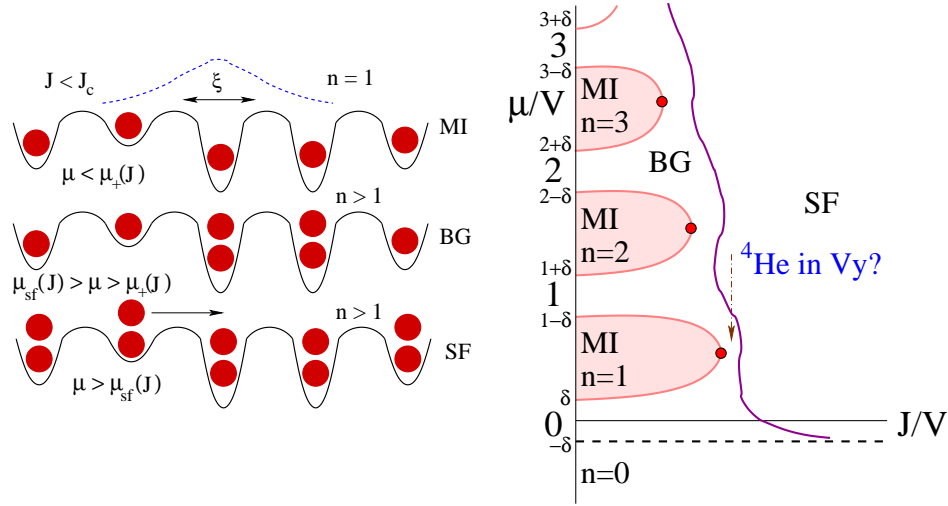


Fig. 3. **Left:** Schematic illustration of lattice bosons near unit filling in the presence of bounded site disorder. If the disorder is not too strong ($\delta \equiv \Delta/V < \frac{1}{2}$), there is still a (shrunk) Mott lobe with a finite energy gap for adding or removing particles. Unlike in the pure case (Fig. 2), superfluidity is not generated immediately outside this lobe. For sufficiently small $n - 1$, the additional particles are Anderson localized by the residual random background potential of the effectively inert layer. A finite compressibility distinguishes this new insulating Bose glass (BG) phase from the MI. The superfluid critical point $\mu_{sf}(J)$ occurs only once the added particles have sufficiently smoothed the background potential that its effective lowest lying single particle states become extended. **Right:** Associated phase diagram, with MI, BG and SF phases. The transition to superfluidity is always from the BG phase, is in the same universality class along the entire transition line, and is ultimately the correct description of helium in Vycor.

3.2. Disordered system

Consider now the addition of site disorder. The left panel of Fig. 3 motivates the existence of a third phase, the Bose glass (BG) phase,^d that intervenes between the Mott and superfluid phases.⁷ Beginning again with the $J = 0$ limit, for sufficiently bounded disorder, $\Delta < V/2$, there remains an interval $(n_0 - 1)V + \Delta < \mu < n_0V - \Delta$ over which every site still has exactly n_0 particles. However, for μ just outside this interval, some sites will have an extra particle (or hole), and the fraction of such sites will vary continuously with μ —even at $J = 0$ the state is now compressible.

For small J , there will still be an interval $\mu_c^-(J, \Delta, n_0) < \mu < \mu_c^+(J, \Delta, n_0)$ where mutual repulsion continues to dominate the disorder, and the incompressible Mott lobe, though shrunk, still survives (right panel of Fig. 3). A rare region argument will be used in Sec. 4 to show that $\mu_{\pm}(J, \Delta, n_0) = \mu_{\pm}(J, 0, n_0) \mp \Delta$ are

^dThe term “Bose glass” may have originated in the early work of Ref. 25, who studied a Hartree-Fock approximation to (1). It transpires that such an effective single-particle treatment of the interactions is a very poor approximation for disordered bosons, and their main conclusions were disputed in Ref. 26.

10 *Peter B. Weichman*

simple translates of those of the clean system (Fig. 5).

The compressible phase just outside the Mott lobe, however, can no longer be a superfluid. The extra particles (or holes) propagating atop the background Mott phase now encounter a background random potential, and the usual Anderson arguments⁵ show that the low energy effective single particle states must be localized, and the state therefore remains insulating. Only after a sufficient density of particles has been added, $\mu > \mu_{\text{sf}}(J)$, is the residual random potential sufficiently smooth that the lowest lying state becomes extended, and the transition to superfluidity takes place. Note the key role here of the pair interactions that allow particles to gradually “fill in” the deeper minima in the background potential.

Note that for $\Delta > V/2$ (which includes unbounded, e.g., Gaussian, disorder) the Mott lobes are entirely destroyed, and only the Bose glass and superfluid phases survive. This is presumably the case for helium in Vycor, where the pore irregularities are too strong to permit a Mott phase.

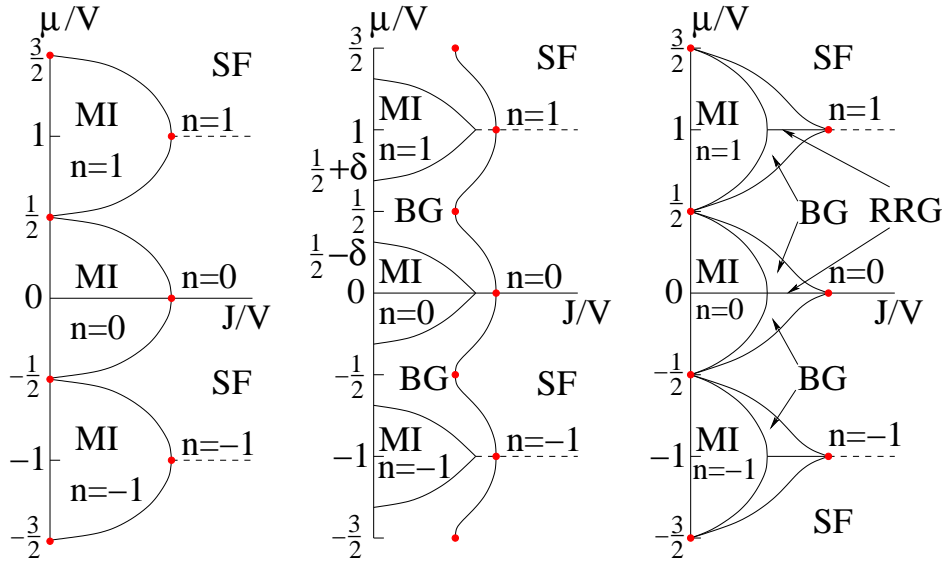


Fig. 4. Schematic phase diagrams for the Josephson junction model (adapted from Ref. 27). Periodicity in μ/V is evident. Even site energy distributions have also been assumed, hence the symmetry under $\mu \rightarrow -\mu$ as well. **Left:** Clean case. **Center:** Generic site-disordered case, with $\delta = \Delta/V$. **Right:** Case of pure hopping disorder. The compressible Bose glass (BG) is replaced an incompressible random rod glass (RRG) on the special lines at integer filling. The penetration of the superfluid phase all the way to $J = 0$ at half-integer filling may be understood via a mapping to a spin- $\frac{1}{2}$ quantum planar XY model with random exchange, but vanishing out-of-plane magnetic field.²⁷

3.3. Phase diagrams for the Josephson junction model

For comparison, phase diagrams for the Josephson junction model are shown in Fig. 4. The clean and site disordered models (left and center panels) are essentially identical to their Bose-Hubbard counterparts (Figs. 2 and 3, respectively), except for the periodicity in μ/V , and symmetry under inversion $\mu \rightarrow -\mu$ for evenly distributed u_i (reflecting the existence of an exact, rather than effective, particle-hole symmetry).

On the other hand the case of pure hopping disorder (right panel of Fig. 4) has no Bose-Hubbard analogue. In the absence of an exact particle-hole symmetry, random J_{ij} always produces, in a renormalization group sense, an effective random site energy even if none is present in the original model—hence the choice of nonrandom J in (1). The exact particle-hole symmetry for integer and half-integer μ/V drastically changes the character of the model along these lines. For integer $\mu/V = n_0$, although the Mott gap closes at a finite value $J = J_M$, the random rod glass (RRG) phase (see Sec. 5) beyond it is incompressible. However, instead of vanishing over a finite interval, for $J > J_M$ the compressibility is finite for any $\mu/V \neq n_0$ (thus indicating a Bose glass phase), and vanishes with an essential singularity, $\sim e^{-c_0/|\mu/V - n_0|}$, as $|\mu/V - n_0| \rightarrow 0$.²⁷ There are corresponding stretched exponential tails, as opposed to the Mott phase linear exponential tail, in the temporal correlation function.²⁷

At half-integer μ/V the particle-hole symmetry has a different effect, eliminating the glassy phase for all nonzero J . The model may be mapped to a spin- $\frac{1}{2}$ quantum XY model, with the u_i corresponding to mean-zero z -axis magnetic fields. If $u_i \neq 0$, then for sufficiently small J it is energetically favorable for a large fraction of the spins to align with the field along z , destroying the in-plane ferromagnetic order that signifies superfluidity—this is the Bose glass phase. Only if $u_i \equiv 0$ can the in-plane order, at least in higher dimensions $d > 1$,^e be maintained for arbitrarily small exchange coupling.

4. Droplet model of the Bose glass phase and the MI–BG phase boundary

Before describing more formal theoretical approaches, I turn here to some very simple arguments that provide a more intuitive picture of the Bose glass phase, determine the exact vertical width of MI–BG phase boundary (Fig. 5), and establish essentially rigorously that there can never be a direct MI–SF transition. As in the clean case, for given J, n_0 the Mott phase is insensitive to μ , and described a unique ground state wavefunction. The phase boundary again occurs when μ coincides with the lowest lying single particle (or hole) excitation $\mu_{\pm}(J, \Delta, n_0) = \pm[E(n_0 N_L \pm 1, \Delta, J) - E(n_0 N_L, \Delta, J)]$. The nature of these excitations, and thereby the values

^eFor a strong-disorder approach to the 1D problem, complementary to the weak disorder limit treated by Kosterlitz-Thouless-type theories, see Refs. 28, 29.

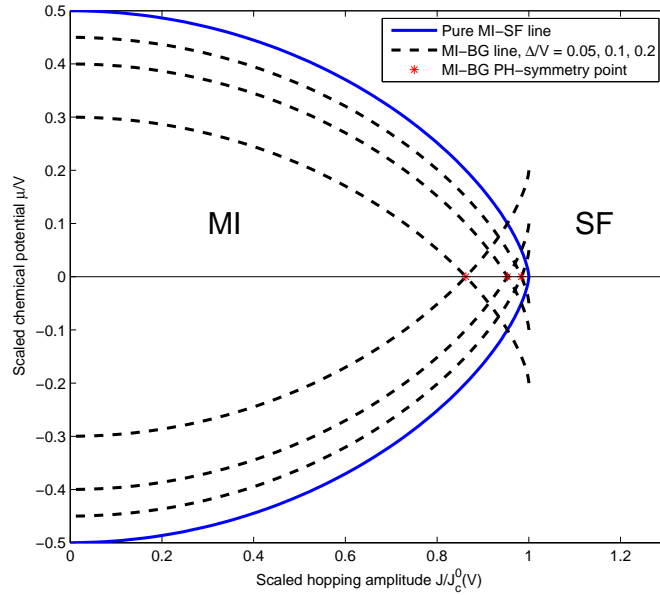


Fig. 5. Sketch of the Mott lobe boundaries as a function of the disorder (adapted from Ref. 27). For simplicity, we consider here the $n_0 = 0$ lobe of the Josephson junction model, for which $\mu_+ = -\mu_-$. The phase boundaries are simply those of the pure system translated inwards by the disorder distribution half-width Δ : $\mu_{\pm}(J, \Delta) = \mu_{\pm}(J, 0) \mp \Delta$. The result, for example, is a corner, or slope discontinuity, at the Mott lobe tip $J_M(\Delta)$ satisfying $\mu_+(J_M, 0) - \mu_-(J_M, 0) = 2\Delta$ (marked by stars).

of μ_{\pm} , will now be established.

4.1. Low-lying particle and hole excitations

Consider the addition of a single particle to the system. The energy required can never be less than it would be if all site energies were as small as possible, $u_i = -\Delta$ for all i . This situation is equivalent to a simple shift, $\mu \rightarrow \mu - \Delta$, and the bound $\mu_+(J, \Delta, n_0) \geq \mu_+(J, 0, n_0) - \Delta$ follows immediately. On the other hand, with an exponentially small density, scaling as $p(R) \sim e^{-[R/R_0(\delta)]^3}$, where R_0 is some length scale depending on the precise distribution of the u_i , there will be rare, isolated “droplets” enclosing a sphere of arbitrarily large radius R , on which all $u_i \leq -\Delta + \delta u$ are nearly uniform, and within an arbitrarily small energy δu of $-\Delta$. The single particle excitation energy of such a droplet (above the uniform $u_i = -\Delta$ value) scales as $\delta \varepsilon \approx c_1 \delta u + c_2 J(d/R)^2$, where c_1, c_2 are appropriate geometrical constants, and the second term represents the ground state of a particle in a box of radius

R .^f In an infinite system, both terms can be made as small as one wishes, and one obtains the opposite inequality $\mu_+(J, \Delta, n_0) \leq \mu_+(J, 0, n_0) - \Delta$. One therefore concludes that $\mu_+(J, \Delta, n_0) = \mu_+(J, 0, n_0) - \Delta$, and by an identical argument for the hole excitations, that $\mu_-(J, \Delta, n_0) = \mu_-(J, 0, n_0) + \Delta$: the upper and lower pure system phase boundaries each simply translate inwards by Δ . This result is sketched in Fig. 5. The tip of the Mott lobe occurs at the point $J = J_M(\Delta, n_0)$ where the two curves intersect, i.e., $\mu_+(J_M, 0, n_0) - \mu_-(J_M, 0, n_0) = 2\Delta$, thereby replacing the critical singularity at $J_c, \Delta = 0$ by a simple slope discontinuity.

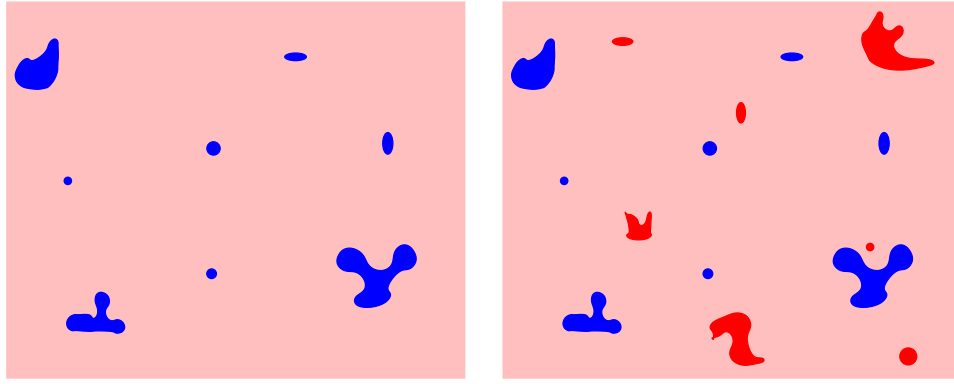


Fig. 6. Schematic illustration of the droplet model of the Bose glass phase for the random site energy model (adapted from Ref. 27). **Left:** Exiting the Mott lobe at fixed $J < J_M$ below its tip with increasing $\mu > \mu_+(J, \Delta)$ [or decreasing $\mu < \mu_-(J, \Delta)$]. For arbitrarily small $\epsilon = \mu - \mu_+(J, \Delta)$ there will be an (exponentially small) density of droplets with volume large enough that the energy gap to adding a particle is smaller than ϵ . **Right:** Exiting the Mott lobe from its tip at fixed μ with increasing $J > J_M$. For arbitrarily small $\Delta J = J - J_M(\Delta)$ there will similarly be arbitrarily large droplets whose local chemical potential magnitude is above the energy gap required to add a particle (previous droplets from the left illustration), or below that required to remove a particle (additional droplets).

4.2. Superfluid droplets and the Bose glass phase

Now, as μ increases above μ_+ (or decreases below μ_-), these excitations begin to be populated with particles (or holes)—the system is compressible. As sketched in Fig. 6, the droplets now behave like uniform dilute superfluid regions just above or below the clean system phase boundary. As illustrated in somewhat more detail in Fig. 7, particles enter a given droplet at discrete values of increasing μ , with gaps controlled by the droplet volume and the bulk compressibility of the clean system. Although the droplets are superfluid, they are (exponentially in $1/|\mu - \mu_{\pm}|$) widely

^fMore correctly, for larger J , one should replace Jd^2 in the second term of $\delta\epsilon$ by a quantity scaling with the background correlation length $\xi(J)$.

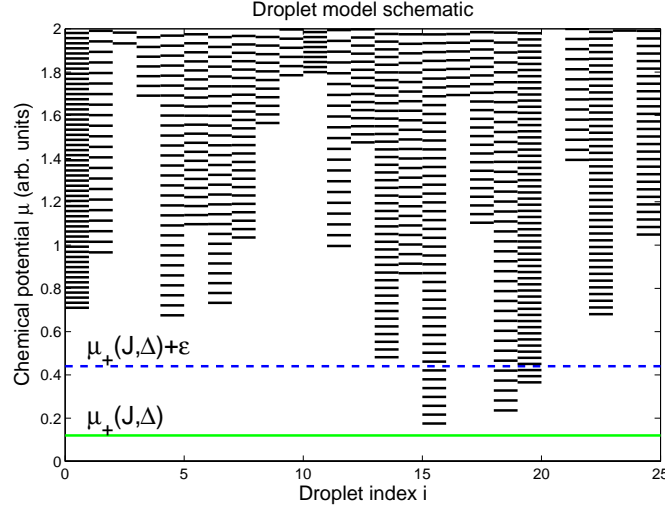


Fig. 7. Schematic illustration of spectrum of droplet excitations (adapted from Ref. 27). Droplets are assumed to be well separated, and independent (see Fig. 6). The horizontal axis is an arbitrary droplet index. The vertical axis shows the critical chemical potential levels (in arbitrary units) at which a new particle is added for each droplet. The lower bound of the excitation spectrum lies at the Mott phase boundary $\mu_+(J, \Delta) = \mu_+(J, 0) - \Delta$ (solid horizontal line). For any $\epsilon \equiv \mu - \mu_+ > 0$ (dashed horizontal line), there will be a finite (but exponentially small) density of large droplets with local chemical potential lying sufficiently far above μ_+ that one or more extra particles are added. The total number of particles added is given by counting the number of “occupied” levels below μ . For a given droplet, while the lowest excitation depends primarily on the local chemical potential, subsequent particles are added in sequence, with gaps scaling as $1/\kappa_+ V$ where V is the droplet volume, and $\kappa_+(J, \mu_+)$ is the bulk compressibility of the pure (superfluid) phase just above the Mott phase boundary. In an infinite system there are infinitely many droplets, implying a continuous distribution of excitation energies, and the bulk density will increase continuously with increasing $\epsilon > 0$.

separated. Global superfluid long range order would require that the particles be able to tunnel coherently through the intervening Mott phase, producing a finite (but, at best, exponentially small) superfluid density. Such would indeed be the case, for example, for identical droplets arranged periodically in a homogeneous background. However, in the present case, the tunneling particle also experiences a residual random potential due to the u_i (suitably renormalized by many body effects in the Mott background), and the usual Anderson localization arguments imply that phase coherence cannot be maintained.

A similar argument pertains if one exits the Mott lobe near its tip, by increasing $J > J_M$ at fixed μ . In this case there are simultaneously present an exponentially dilute [in $1/(J - J_M)$] set of both particle and hole superfluid droplets (right panel of Fig. 6). By the same Anderson localization argument, neither set of droplets can support global phase coherence.

In summary, one concludes that a new compressible, insulting Bose glass phase

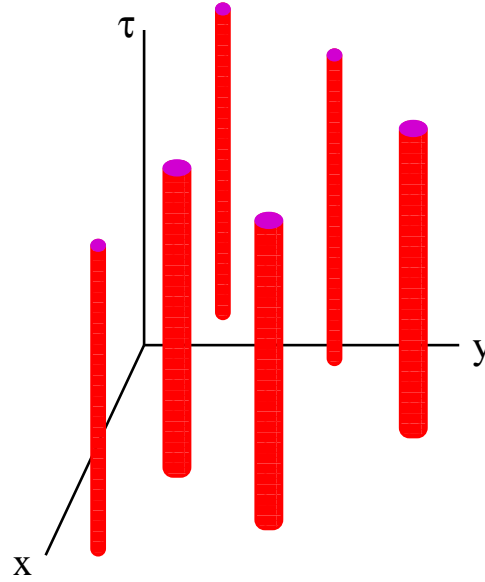


Fig. 8. Schematic illustration of random rod-like structure generated by quenched disorder in quantum models (adapted from Ref. 27). The cylinders represent, for example, random regions of enhanced or suppressed hopping strength or site energies.

completely surrounds the Mott lobe, and a direct MI–SF transition is impossible. However, as $|\mu - \mu_{\pm}|$ (or $J - J_M$) increases further, the superfluid droplets grow in size, and new ones are created (as μ overcomes larger and larger local u_i values). Eventually they percolate sufficiently that global phase coherence is stabilized, and a BG–SF transition takes place. This transition is presumably the ultimate zero temperature description of helium in Vycor.

5. Path integral formulations and universality classes

Given now a basic understanding of the underlying physics of the MI, BG and SF phases, I turn now to more formal treatments that allow one to clearly identify possible universality classes, and their coarse-grained field theoretic descriptions. One begins with the path integral representation, based on the Trotter decomposition of the partition function of the Josephson function model (2), $Z = \int D\phi e^{-\mathcal{L}_J}$ with Lagrangian:²⁷

$$\mathcal{L}_J[\phi] = \int_0^\beta d\tau \left\{ - \sum_{i,j} J_{ij} \cos[\phi_i(\tau) - \phi_j(\tau)] + K \sum_i [\partial_\tau \phi_i + i(u_i - \mu)]^2 \right\} \quad (5)$$

in which $\beta = 1/k_B T \rightarrow \infty$, $K = 1/2V$, and $-\infty < \phi_i(\tau) < \infty$ are continuous classical phase fields. As usual, the quantum degrees of freedom give rise to an extra (imaginary time) dimension τ in the effective classical model. In general this

extra dimension is highly anisotropic, and, except in special cases, does *not* simply lead to the same classical model in one higher dimension. It is immediately evident, for example, that the disordered quantities J_{ij}, u_i are τ -independent. The point like quenched disorder in the quantum model therefore leads to a picture of *columnar* or *rod-like* disorder in the classical model (Fig. 8).

In order to place (5) in the context of more familiar field theoretic models, we develop a coarse-grained, long wavelength continuum approximation to (5). Let $e^{i\phi_i(\tau)} \rightarrow \psi(\mathbf{x}, \tau)$, and relax the sharp condition $|\psi| = 1$ on the field magnitude in the standard fashion by adding terms $\frac{1}{2}r_0|\psi|^2 + \frac{1}{4}u_0|\psi|^4$ to \mathcal{L} (which constrains $|\psi| \approx \sqrt{-r_0/u_0}$). In addition the cosine term is approximated by a squared gradient term $J|\nabla\psi|^2$. The result is an effective ψ^4 Lagrangian,

$$\mathcal{L}_c[\psi] = \int_0^\beta d\tau \int d^d x \left\{ \frac{1}{2}|\nabla\psi|^2 - \frac{1}{2}\psi^*[\partial_\tau - g(\mathbf{x})]^2\psi + \frac{1}{2}r(\mathbf{x})|\psi|^2 + \frac{1}{4}u_0|\psi|^4 \right\}. \quad (6)$$

Space and time have been rescaled so that the squared derivative terms have unit coefficient. The random J_{ij} is then subsumed into a random $r(\mathbf{x}) = r_0 + \delta r(\mathbf{x})$, and $-\mu + u_i$ has been subsumed into a random $g(\mathbf{x}) = g_0 + \delta g(\mathbf{x})$, with $\langle \delta r \rangle = \langle \delta g \rangle = 0$. Superfluidity corresponds to a nonzero anomalous average $\langle \psi \rangle$, and one may think of r_0 as the control parameter which takes one from the normal phase for large positive r_0 , to the superfluid phase for large negative r_0 .

One may now consider the various possible classes of phase transition depending on the various terms, and their underlying symmetries, that one keeps in (6). Table 1 lists the relevant special cases.

5.1. Particle-hole symmetric transitions

The particle-hole symmetric model $\mu = 0, u_i \equiv 0$ corresponds to $g(\mathbf{x}) \equiv 0$. The Lagrangian \mathcal{L}_0 (clean system) or \mathcal{L}_2 (system with random hopping) is then purely real, and $e^{-\mathcal{L}_{0,2}}$ may be interpreted in terms of a classical probability density for the two-component field $(\text{Re}(\psi), \text{Im}(\psi))$. The squared-gradient interaction in both space and time implies that the model is the usual Landau-Ginzburg-Wilson representation of a ferromagnetic XY-model in $(d+1)$ -dimensions. In the clean case, time and space are fully symmetric, and the transition (through the tips of the Mott lobes in Fig. 2) is in the universality class of the usual classical $(d+1)$ -dimensional XY model. With random hopping, $\delta r(\mathbf{x}) \neq 0$, strong anisotropy is generated by the columnar disorder (see Fig. 8), and the transition is in the universality class of the so-called *classical random rod problem*.^{30,31,32}

5.2. Particle-hole asymmetric transitions

For nonzero μ or u_i , hence $g(\mathbf{x})$, the Lagrangian is complex, and a classical probabilistic interpretation is no longer possible. The leading interaction is now a (purely imaginary) linear time derivative $g\psi^*\partial_\tau\psi$, which generates an even stronger space-time anisotropy. For the clean system, $g_0 \neq 0$ but $\delta r(\mathbf{x}) = \delta g(\mathbf{x}) \equiv 0$ (the

Pure PH-sym [(d + 1)-dimensional XY model]:

$$\mathcal{L}_0 = \int d^d x \int d\tau \left\{ \frac{1}{2} |\nabla \psi|^2 + \frac{1}{2} |\partial_\tau \psi|^2 + \frac{1}{2} r_0 |\psi|^2 + \frac{1}{4} u_0 |\psi|^4 \right\}$$

Pure PH-asym [d-dimensional dilute Bose gas]:

$$\mathcal{L}_1 = \int d^d x \int d\tau \left\{ \frac{1}{2} |\nabla \psi|^2 - \frac{1}{2} \psi^* (\partial_\tau - g_0)^2 \psi + \frac{1}{2} r_0 |\psi|^2 + \frac{1}{4} u_0 |\psi|^4 \right\}$$

PH-sym RR [(d + 1)-dimensional classical random rod model]:

$$\mathcal{L}_2 = \int d^d x \int d\tau \left\{ \frac{1}{2} |\nabla \psi|^2 + \frac{1}{2} |\partial_\tau \psi|^2 + \frac{1}{2} [r_0 + \delta r(\mathbf{x})] |\psi|^2 + \frac{1}{4} u_0 |\psi|^4 \right\}$$

PH-asym RR [(d + 1)-dimensional incommensurate random rod model]:

$$\mathcal{L}_3 = \int d^d x \int d\tau \left\{ \frac{1}{2} |\nabla \psi|^2 - \frac{1}{2} \psi^* (\partial_\tau - g_0)^2 \psi + \frac{1}{2} [r_0 + \delta r(\mathbf{x})] |\psi|^2 + \frac{1}{4} u_0 |\psi|^4 \right\}$$

Statistical PH-sym [commensurate dirty boson problem]:

$$\mathcal{L}_4 = \int d^d x \int d\tau \left\{ \frac{1}{2} |\nabla \psi|^2 - \frac{1}{2} \psi^* [\partial_\tau - \delta g(\mathbf{x})]^2 \psi + \frac{1}{2} [r_0 + \delta r(\mathbf{x})] |\psi|^2 + \frac{1}{4} u_0 |\psi|^4 \right\}$$

Generic PH-asym [incommensurate dirty boson problem]:

$$\mathcal{L}_5 = \int d^d x \int d\tau \left\{ \frac{1}{2} |\nabla \psi|^2 - \frac{1}{2} \psi^* (\partial_\tau - g_0 - \delta g(\mathbf{x}))^2 \psi + \frac{1}{2} [r_0 + \delta r(\mathbf{x})] |\psi|^2 + \frac{1}{4} u_0 |\psi|^4 \right\}$$

Table 1. Continuum ψ^4 representation of models with various types of disorder and various degrees of particle-hole symmetry. The coefficients of $|\nabla \psi|^2$ and $|\partial_\tau \psi|^2$ have been normalized to $\frac{1}{2}$. The control parameters r_0 and g_0 are analogous to J_0 and μ , respectively. Disorder in the hopping strengths is represented by δr , while that in the site energies is represented by δg . Both are independent of τ , and in field theoretic treatments, are taken as quenched Gaussian random fields with zero mean and delta-function correlations characterized by variances Δ_r and Δ_g , respectively. Disorder in the other parameters (including the unit gradient-squared coefficients) may also be introduced, but produces no new critical behavior.

Lagrangian \mathcal{L}_1), this term generates critical behavior equivalent to the onset of superfluidity (described quantitatively by the Bogoliubov model^g at zero density in a dilute Bose gas.^h

If $g_0 = 0$ and $\delta g(\mathbf{x}) \neq 0$ has an even distribution, then the corresponding Lagrangian \mathcal{L}_4 has a *statistical particle-hole symmetry*—the $g\psi^*\partial_\tau\psi$ term is locally nonzero, but zero on average (the manifestation of this symmetry is more evident in the replicated, disorder averaged Lagrangian discussed in Sec. 7). It will be argued below that the transition in this case is identical to that for the generic Lagrangian \mathcal{L}_5 in which all terms are nonzero, so that the statistical symmetry is *restored* at the critical point.ⁱ Intuitively, the expanding superfluid droplets in the Bose glass

^gSee, e.g., Ref. 33. For a more modern view, see Ref. 14.

^hThe usual coherent state functional integral formulation of the boson model (1) corresponds to an *absent* $|\partial_\tau \psi|^2$ term, and a *unit coefficient* $\psi^*\partial_\tau\psi$ term, so that the model can never possess an exact particle-hole symmetry. Treating both particle-hole symmetric and asymmetric models requires the expanded space of Lagrangians corresponding to (6).

ⁱThis idea has been used to explain the vanishing of the Hall conductivity at magnetic field-tuned

phase as the superfluid phase boundary is approached lead to a decoupling of the particle number from the lattice potential. The discrete droplet excitation spectrum pictured in Fig. 7, which replaces the individual lattice site occupation spectrum, becomes denser and denser, the statistics of the energy spectrum loses its up-down asymmetry, and there is less and less distinction between the statistics of particle and hole excitations as μ is varied.

Less surprisingly, the particle-hole asymmetric random rod model, \mathcal{L}_3 , in which $g_0, \delta r(\mathbf{x}) \neq 0$ but $\delta g(\mathbf{x}) \equiv 0$, is equivalent to the generic model. In the renormalization group sense, the combined effect of g_0 and $\delta r(\mathbf{x})$ produces nonzero $\delta g(\mathbf{x})$. Intuitively, in the original boson model (1), random hopping produces regions of varying compressibility, and a uniform μ will produce a nonuniform density. As far as critical behavior goes, this is indistinguishable from density fluctuations produced a random site potential (Sec. 4 and Figs. 6, 7).

6. Quantum scaling theory

In describing the Vycor data in Sec. 1 several zero temperature critical exponents were introduced. Here the general scaling theory of a QPT (which is not initially limited to the dirty boson problem) is summarized, these exponents are placed in a more general context, and scaling relations between them and more familiar exponents are derived.⁷

Let δ be the thermodynamic control parameter (e.g., $J - J_c$, $\mu - \mu_c$, or $r_0 - r_{0,c}$), with critical point at $\delta = 0$. The divergence of the spatial and temporal correlation lengths, $\xi \approx \xi_0 |\delta|^{-\nu}$, $\xi_\tau \approx \xi_{0,\tau} |\delta|^{-\nu_\tau}$ define critical exponents ν, ν_τ . The *dynamical exponent* $z = \nu_\tau / \nu$ quantifies the space-time anisotropy. In particular, the isotropic Lagrangian \mathcal{L}_0 must lead to $z = 1$, while for the remaining models one expects $z \neq 1$. The singular part of the free energy scales in the form $F_s \approx A |\delta|^{2-\alpha}$, which defines the analogue of a zero temperature “specific heat” exponent α . The *quantum hyperscaling* relation $2 - \alpha = (d + z)\nu$ follows from the assumption that F_s , being an energy density, scale also inversely with the space-time correlation volume $(\xi_\tau \xi^d)^{-1} \approx (\xi_{\tau,0} \xi_0^d)^{-1} |\delta|^{(d+z)\nu}$.

The critical behavior of the superfluid density, $\rho_s \approx \rho_{s,0} |\delta|^\nu$ defines an exponent ν . The superfluid density is a torsional modulus quantifying the stiffness of the order parameter, and is therefore derived from the free energy increment $\Delta F_s = \frac{1}{2} \rho_s v_s^2$ (which must be part of F_s because ρ_s vanishes in the insulating phase, and is therefore a singular quantity), where the superfluid velocity $\mathbf{v}_s = \hbar \mathbf{k}_s / m$ is generated by a long wavelength gradient $\mathbf{k}_s = \nabla \phi$ in the order parameter phase (corresponding to a helical twist in the order parameter itself). Since \mathbf{k}_s is an inverse length, it must scale as ξ^{-1} , and one obtains the *quantum Josephson relation* $\nu = 2 - \alpha - 2\nu = (d + z - 2)\nu$. If, as in the Vycor experiments, one uses the particle density difference as the control parameter, $\delta = \rho - \rho_c$, then the exponent ω defined

in Fig. 1 is given simply by $\omega = \nu$.

The temperature is similarly included via the temporal finite size scaling form $F_s \approx A|\delta|^{2-\alpha}Y(\beta/\xi_\tau)$, in which $Y(y)$ is a universal scaling function with $Y(\infty) = 1$. For finite β the argument is finite, and $Y(y)$ must interpolate between the zero and finite temperature critical behaviors. In particular, the finite temperature transition must occur at some value $y = y_c$, which leads to the relation $k_B T_c(\delta) \approx (y_c \xi_{\tau,0})^{-1} |\delta|^{z\nu}$. Referring again to Fig. 1, one therefore obtains $\rho_s(T = 0) \sim T_c^\theta$ with $\theta = (d + z - 2)/z$. One obtains therefore the ratio $\omega/\theta = z\nu = \nu_\tau$.

Using the Vycor data experimental values $\omega = 1.7 \pm 0.3$ and $\theta = 1.25 \pm 0.2$ in $d = 3$, one obtains the reasonable result $\nu_\tau = 1.4 \pm 0.3$. However, the implied relations $z = 1/(\theta - 1)$ and $\nu = \omega/\theta z$ produce the remarkably unsatisfactory bounds $2.2 \leq z \leq 20$ and $0.07 \leq \nu \leq 0.64$. Unfortunately, more accurate bounds would require much higher quality data, but even with the intervention of 25 years, the original experiments⁸ would be extremely difficult to improve upon.

6.1. Compressibility and z vs. d

If one uses $\delta = \mu - \mu_c$, the compressibility $\kappa = \partial n / \partial \mu = -\partial^2 F / \partial \delta^2$ has a singular part $\kappa_s \sim |\delta|^{-\alpha}$ controlled by the zero temperature specific heat exponent (this is true more generally so long as variation in δ leads to variation in the density). However, the *total* compressibility also has an interpretation as a *temporal superfluid density*: the free energy increment due to temporal phase twists $\omega_s = \partial_\tau \phi$ is given by $\Delta F_\tau = \frac{1}{2} \kappa \omega_s^2$. This identification follows from (5) since the imposition of the phase twist ω_s is equivalent to the shift $\mu \rightarrow \mu + i\omega_s$, and it follows that $\partial^2 \Delta F_\tau / \partial \omega_s^2 = -\partial^2 F / \partial \mu^2 = \kappa$. By analogy to ρ_s , if one assumes that ΔF_τ is part of F_s , and proposes that ω_s scales as ξ_τ^{-1} , then one obtains $\kappa \approx \kappa_0 |\delta|^{v_\tau}$ with $v_\tau = (d - z)\nu$. The physical fact that κ is finite and nonzero through the transition (with κ_s yielding a small correction since one expects $\alpha < 0$) then leads to the proposed scaling relation $z = d$.⁷

However, this argument lies on very shaky ground because it is difficult to reconcile κ_s and κ obeying separate critical scaling relations. In fact, the difference $\kappa - \kappa_s$, being finite through the BG-SF transition, is dominated by the analytic background, and ΔF_τ should be likewise.³⁶ Moreover, since the shift $\mu \rightarrow \mu + i\omega_s$ simply leads to a small adjustment of a parameter that is already nonzero, the scaling assumption $\omega_s \sim \xi_\tau^{-1}$ is inappropriate. *Only if* $\mu = 0$, $u_i \equiv 0$, so that ω_s breaks particle-hole symmetry, should one expect such a scaling.^j Indeed, for the random rod problem, $\kappa = \kappa_s$ is entirely singular since, like ρ_s , it vanishes identically in the RRG phase. Consistently, one finds $v_\tau > 0$, hence $z < d$, at that

^jFor ρ_s , the spatial phase twist corresponds to the shift $\nabla^2 \rightarrow (\nabla + i\mathbf{k}_s)^2$, introducing a momentum term $i\mathbf{k}_s \cdot \psi^* \nabla \psi$ which breaks a spatial inversion symmetry. It is for this reason that one expects the critical scaling of k_s with ξ^{-1} .

transition.^{30,31,32} Consistently as well, the control parameter $\delta = J - J_c$ in that case does not couple to the density, and κ is no longer related to the exponent α .

In conclusion, at both the RR-SF and BG-SF transitions z is expected to remain an independent exponent, undetermined by any simple scaling relation. Recent high resolution quantum Monte Carlo simulations in $d = 2$ support this view, finding $z = 1.40 \pm 0.02$ at the BG-SF transition.³⁷

6.2. Universal critical sheet conductance in $d = 2$

The conductivity is related to the superfluid density via the zero frequency limit of $\sigma = \rho_s / i\omega$. If one assumes that ω , being an inverse time, scales as ξ_τ^{-1} (this is reasonable here, because ω is a real dynamic frequency, not an imposed phase twist, and σ is indeed singular), one obtains $\sigma \approx \sigma_0 |\delta|^\Sigma$ with $\Sigma = 2 - \alpha - (z+2)\nu = (d-2)\nu$. This has the remarkable implication that, very generally, in $d = 2$ the conductivity, while vanishing in the insulating phase, and diverging in the superfluid phase, has a *finite constant* value σ_c right at the critical point. Experiments on disordered superconducting thin films, where δ is the film thickness or an applied magnetic field, provide some support for this^{38,39,40} (see also Ref. 41 and references therein). Moreover, *quantum hyperuniversality*,⁴² which predicts not only that the critical exponents for F_s and $(\xi_\tau \xi^d)^{-1}$ coincide, but also that the amplitude combination $F_s \xi_\tau \xi^d \approx A \xi_{\tau,0} \xi_0^d$ also be a universal number, predicts that $\sigma_c = A \xi_{\tau,0} \xi_0^2$ coincides with this amplitude, and therefore should be *universal*.^k This has much less experimental support—a large range of estimated σ_c values are found.^{38,39,41} On the other hand, critical amplitude ratios are far more difficult to measure accurately than critical exponents, and higher quality data would again be desirable.

7. Renormalization group approaches

The dirty boson problem has so far discussed from a phenomenological point of view, emphasizing elementary excitations, symmetry principles, and results that follow from general scaling relations. This review is concluded with a brief survey of renormalization group approaches to quantitative evaluation of exponents and other quantities.

7.1. One-dimensional models

There is one limit where exact solutions exist, namely $d = 1$.^{44,45,7,28,29} The model maps to a classical 2D fluctuating sine-Gordon-type interface roughening

^kThe scaling theory is general, and does not require any identification between the dirty superconducting and superfluid systems. However, in modeling thin films close to the transition, it is typically argued that Cooper pairs may indeed be treated as bosons, hence that the transition lies in the same universality class as the dirty boson problem, and σ_c may be computed within this model. See, e.g., Ref. 43.

model:²⁷

$$\mathcal{L}_{\text{SG}}[\mathbf{h}] = \int dx \int d\tau \left\{ \frac{1}{2} K(x) (\partial_\tau h)^2 + \frac{1}{2} V(\partial_x h)^2 - m(x) \partial_x h - 2y_0 \cos(2\pi h) \right\}, \quad (7)$$

where $h(x, \tau)$ is the interface height at a given space-time point.¹ The hopping disorder leads to disorder in the interface tension coefficient $K(x)$, while the chemical potential and site disorder leads to the disordered tilt potential $m(x) = m_0 + \delta m(x)$. The cosine term prefers integer values of h , a reflection of the original integer boson site occupancy. At sufficiently large y_0 this term pins the interface at a fixed integer height, with small fluctuations about it. This is the Mott insulating phase. For the 1D random rod problem, $m(x) \equiv 0$, at small y_0 the fluctuations are able to unpin the interface, leading to logarithmically divergent large scale fluctuations: this corresponds to the superfluid phase. The disorder in K turns out to be irrelevant at this transition, so both the clean and random rod problems are described by the usual classical 2D Kosterlitz-Thouless theory, with, in particular $z = 1$ and critical correlation decay exponent $\eta = \frac{1}{4}$ (see, e.g., Ref. 47).

On the other hand, nonzero $m(x)$ couples directly to the interface slope, and can have a much stronger effect. At a sufficiently large average value, m_0 , there is a transition to an interface with an average constant spatial tilt. The value of m_0 at the onset of this tilt corresponds to the Mott excitation gap. For sufficiently small K, V the fluctuations about the mean tilt completely wash out the cosine term and are again logarithmically divergent on large scales: this is again the superfluid phase. However, at intermediate values there is enough residual effect of the cosine term to constrain the interface to finite fluctuations about this tilted state—this corresponds to the Bose glass phase. The BG–SF transition is described by a modified Kosterlitz-Thouless theory^m which produces different universal critical properties.^{44,45,7} For example, although $z = 1$ still, one now finds $\eta = \frac{1}{3}$. Moreover, near the transition one may absorb m_0 into a shift $h \rightarrow h - (m_0/V)x$, so that only δm enters. This explicitly demonstrates the asymptotic restoration of statistical particle-hole symmetry in the 1D model.

7.2. Epsilon-expansions in higher dimensions

We now turn to epsilon-expansion type approaches in higher dimensions that have proven so useful in quantifying classical critical phenomena. Renormalization group

¹An extension to $d = 1 + \epsilon$ dimensions has also been proposed, based on inserting the engineering dimensions appropriate to higher d into the one-dimensional RG flows: see Ref. 46. However, in the absence of a form for the surface roughening type Hamiltonian generalizing (7) for noninteger $d > 1$ (the particle-vortex duality transformations used to obtain such models requires integer d), there is presently no rigorous support for this approach.

^mIn the replicated model, the tilt disorder replaces the usual $\cos(2\pi h)$ term by a replica interaction term of the form $\cos\{2\pi[h_\alpha(x, \tau) - h_\beta(x, \tau')]\}$. This term generates renormalization group flows similar to those of classical Kosterlitz-Thouless (Ref. 47) but with sufficiently different geometry that different universal critical properties are produced.

approaches are generally based on “replicated” Lagrangians, in which the disorder has been integrated out at the expense of introducing p copies, ψ_α , $\alpha = 1, 2, \dots, p$ of the original field that all interact with the same quenched disorder $\delta r, \delta g$, but are otherwise independent, with the formal limit $p \rightarrow 0$ taken at the end. Using the standard delta-correlated Gaussian disorder model, with variances Δ_r and Δ_g , the replicated ψ^4 Lagrangian takes the form $\mathcal{L}_C^{(p)} = \mathcal{L}_{C,1}^{(p)} + \mathcal{L}_{C,2}^{(p)}$ with,^{27,48}

$$\begin{aligned} \mathcal{L}_{C,1}^{(p)} &= \sum_{\alpha=1}^p \int_0^\beta d\tau \int d^d x \left\{ \frac{1}{2} |\nabla \psi_\alpha|^2 - \frac{1}{2} \psi_\alpha^* (\partial_\tau - g_0)^2 \psi_\alpha + \frac{1}{2} r_0 |\psi_\alpha|^2 + \frac{1}{4} u_0 |\psi_\alpha|^4 \right\} \\ \mathcal{L}_{C,2}^{(p)} &= -\frac{1}{2} \sum_{\alpha,\beta=1}^p \int_0^\beta d\tau \int_0^\beta d\tau' \int d^d x \left\{ \Delta_r |\psi_\beta(\mathbf{x}, \tau)|^2 |\psi_\alpha(\mathbf{x}, \tau')|^2 \right. \\ &\quad \left. + \Delta_g [\psi_\alpha^* \partial_\tau \psi_\alpha - g_0 |\psi_\alpha|^2](\mathbf{x}, \tau) [\psi_\beta^* \partial_{\tau'} \psi_\beta - g_0 |\psi_\beta|^2](\mathbf{x}, \tau') \right\}. \end{aligned} \quad (8)$$

The disorder average leads to quadratic interactions between the replicas that are of infinite range in τ , a reflection of its columnar character, and this is what generates new critical behavior. The random rod model corresponds to $g_0 = 0$, $\Delta_g = 0$, so that the Lagrangian is separately invariant under reversal of τ and τ' . The case of statistical particle-hole symmetry corresponds to $g_0 = 0$, $\Delta_g > 0$, which leads to a symmetry only under *simultaneous* reversal of τ, τ' .

Now, imagine beginning with the random rod model, and perturbing it in various ways. Nonzero Δ_g leads, in a heuristic Fourier space notation, to a $\Delta_g \omega^2 \psi^4$ correction to the $\Delta_r \psi^4$ term already present. Under naive power counting, since critical fluctuations are dominated by large scales and long times, increasing powers of frequency lead to less important terms, and one would expect the former term to be strongly irrelevant relative to the latter, i.e., that symmetric site disorder should *not* destabilize the RR critical behavior. On the other hand, g_0 introduces a $ig_0 \omega \psi^2$ perturbation, which by power counting dominates the $\omega^2 \psi^2$ term, and *is* expected to lead to new critical behavior. This is certainly confirmed in the clean model, where it generates the crossover from $(d+1)$ -dimensional XY behavior to weakly interacting Bose gas behavior (Sec. 4.1). However, the notion of asymptotic restoration of particle-hole symmetry requires that, in the disordered case, this term ultimately be subdominant to the Δ_g term.

These paradoxes find their resolution in the fact that naive power counting is exact only at Gaussian critical points, and approximately valid only when interactions (terms of order higher than ψ^2) play a small role. If their role is large, then different terms can indeed exchange dominance. In order to explore such notions quantitatively, it is convenient to have a model parameter that, when varied, interpolates between the near-Gaussian and strongly non-Gaussian limits. In classical critical phenomena, this parameter is $\epsilon = 4 - d$: the standard epsilon expansion is based on the fact that the critical behavior is Gaussian for $d \geq 4$, and nearly so for small $\epsilon > 0$. The corresponding approach for problems with columnar disorder requires not only that d be close to four, but also that the dimension ϵ_τ of the

However, for $\epsilon_\tau > \epsilon_\tau^c$ (with $\epsilon_\tau^c = \frac{8}{29}$ to leading order in ϵ_τ), nonlinear terms in the recursion relations dominate the linear ones (the latter reflecting naive power counting), and the RR fixed point becomes unstable to Δ_g , and a new statistically particle-hole symmetric, or commensurate (C), fixed point bifurcates away from

RR. For not too large ϵ_τ both C and RR remain unstable to g_0 , and IC hence remains the globally stable critical fixed point. However, for $\epsilon_\tau > \epsilon_{\tau 1}$ (with $\epsilon_{\tau 1} = \frac{2}{3}$ to leading order) the incommensurate fixed point intersects the $g_0 = 0$ plane, and merges with C. The latter is now completely stable, and is proposed to correspond to the dirty boson fixed point at $\epsilon_\tau = 1$. This provides a detailed scenario by which statistical particle-hole symmetry is restored. However, the fact that ϵ_τ^c , though small, is a finite number means that the fixed point C is not perturbatively accessible in the usual sense, and one should treat the detailed estimates in the vicinity of this fixed point with caution. The value $\epsilon_{\tau 1}$ is even larger, and therefore even more uncertain, and extrapolation of these results to $\epsilon_\tau = 1$ should be treated as, at best, qualitative estimates. The general scenario proposed, however, seems very natural and illuminating.

8. Summary and conclusions

Over the past twenty years, advances in understanding the rich physics of the phases and phase transitions in disordered boson systems has proceeded fruitfully along a number of different fronts, including descriptions of excitations within the different phases,^{7,27} scaling phenomenology for the critical exponents^{7,36} and universal amplitudes,^{34,35,42,43} exact solutions in one dimension,^{28,29,44,45,46} numerical simulations in one and two dimensions,^{17,18,19,20,21,22,37,43} weak hopping expansion work,^{23,24} and approximate renormalization group epsilon expansion approaches in higher dimensions.^{27,48} I have tried here to give a flavor for all of these, emphasizing qualitative features, such as phase diagrams and the importance of particle-hole symmetry,^{27,34,35,48} and making connections to experiment^{8,15,16,38,39,41} where possible. Perhaps the most interesting future development would be quantitative estimates of the BG-SF critical behavior in three dimensions, which appears to be quantitatively accessible only through numerical simulation. This would allow direct comparisons with the Vycor data (at least for those exponents that appear to be reasonably constrained by the data; of course, better experimental helium data, perhaps using other disordered substrates, would be hugely beneficial as well). However, this may have to await future generations of computational capability, as the required system sizes are currently well out of reach.

References

1. J. A. Hertz, Phys. Rev. B **14** (1976)
2. A. B. Harris, J. Phys. C **7**, 1671 (1974)
3. P. B. Weichman and M. E. Fisher, Phys. Rev. B **34**, 7652 (1986).
4. A. J. Leggett, Physica Fennica **8**, 125 (1973).
5. P. A. Lee and T. V. Ramakrishnan, Rev. Mod. Phys. **57**, 287 (1985);
6. T. Belitz and T. R. Kirkpatrick, Rev. Mod. Phys. **66**, 261 (1994).
7. M. P. A. Fisher, P. B. Weichman, G. Grinstein and D. S. Fisher, Phys. Rev. B **40**, 546 (1989).

8. B. C. Crooker, H. Hebral, E. N. Smith, Y. Takano, J. D. Reppy, Phys. Rev. Lett. **51**, 666 (1983).
9. M. H. Anderson, J. R. Ensher, M. R. Matthews, C. E. Wieman, E. A. Cornell, Science **269**, 198 (1995).
10. K. B. Davis, M.-O. Mewes, M. R. Andrews, M. J. Van Druten, D. S. Durfee, D. M. Kurn, W. Ketterle, Phys. Rev. Lett. **75**, 3969 (1995).
11. M. Rasolt, M. J. Stephen, M. E. Fisher, and P. B. Weichman, Phys. Rev. Lett. **53**, 798 (1984);
12. P. B. Weichman, M. Rasolt, M. E. Fisher, and M. J. Stephen, Phys. Rev. B **33**, 4632 (1986).
13. P. B. Weichman, Ph.D. Thesis, Cornell University (1986).
14. P. B. Weichman, Phys. Rev. B **38**, 8739 (1988).
15. D. Jaksch, C. Bruder, J. I. Cirac, C. W. Gardiner, and P. Zoller, Phys. Rev. Lett. **81**, 3108 (1998);
16. M. Greiner, O. Mandel, T. Esslinger, T. W. Hänsch, I. Bloch, Nature **415**, 39 (2002).
17. R. T. Scalettar, G. G. Batrouni and G. T. Zimanyi, Phys. Rev. Lett. **66**, 3144 (1991).
18. W. Krauth, N. Trivedi and D. M. Ceperley, Phys. Rev. Lett. **67**, 2307 (1991).
19. M. Wallin, E. S. Sørensen, S. M. Girvin, and A. P. Young, Phys. Rev. B **49**, 12115 (1994).
20. S. Zhang, N. Kawashima, J. Carlson and J. E. Gubernatis, Phys. Rev. Lett. **74**, 1500 (1995).
21. F. Alet and E. S. Sørensen, Phys. Rev. E **67**, 015701(R) (2003).
22. N. Prokof'ev and B. Svistunov, Phys. Rev. Lett. **92**, 015703 (2004).
23. J. K. Freericks and H. Monien, Europhys. Lett. **24**, 545 (1994).
24. M. Niemeyer, J. K. Freericks, and H. Monien, Phys. Rev. B **60**, 2357 (1999).
25. J. A. Hertz, L. Fleishman and P. W. Anderson, Phys. Rev. Lett. **43**, 942 (1979).
26. A. J. Bray and M. A. Moore, J. Phys. C **15**, L765 (1982).
27. P. B. Weichman and R. Mukhopadhyay, Phys. Rev. B **77**, 214516 (2008).
28. E. Altman, Y. Kafri, A. Polkovnikov, and G. Refael, Phys. Rev. Lett. **93**, 150402 (2004);
29. E. Altman, Y. Kafri, A. Polkovnikov, and G. Refael, Phys. Rev. Lett. **100**, 170402 (2008).
30. S. N. Dorogovtsev, Phys. Lett. **76A**, 169 (1980).
31. Boyanovsky and J. L. Cardy, Phys. Rev. B **26**, 154 (1982); Erratum, Phys. Rev. B **27**, 6971 (1983).
32. I. D. Lawrie and V. V. Prudvikov, J. Phys. C **17**, 1655 (1984).
33. A. L. Fetter and J. D. Walecka, *Quantum Theory of Many Particle Systems* (McGraw Hill, 1971), Chaps. 10, 14.
34. M. P. A. Fisher, Physica A **177**, 553 (1991).
35. A. T. Dorsey and M. P. A. Fisher, Phys. Rev. Lett. **68**, 694 (1992).
36. P. B. Weichman and R. Mukhopadhyay, Phys. Rev. Lett. **98**, 245701 (2007).
37. A. Priyadarshree, S. Chandrasekharan, J.-W. Lee, and H. U. Baranger, Phys. Rev. Lett. **97**, 115703 (2006).
38. D. B. Haviland, Y. Liu and A. M. Goldman, Phys. Rev. Lett. **62**, 2180 (1989).
39. A. F. Hebard and M. A. Paalanen, Phys. Rev. Lett. **65**, 927 (1990).
40. M. P. A. Fisher, Phys. Rev. Lett. **65**, 923 (1990).
41. A. M. Goldman and N. Markovic, Physics Today, November 1998, pp. 39–44.
42. K. Kim and P. B. Weichman, Phys. Rev. B **43**, 13583 (1991).
43. E. S. Sørensen, M. Wallin, S. M. Girvin, and A. P. Young, Phys. Rev. Lett. **69**, 828 (1992).

26 *Peter B. Weichman*

- 44. T. Giamarchi and H. J. Schulz, Europhys. Lett. **3**, 1287 (1987);
- 45. T. Giamarchi and H. J. Schulz, Phys. Rev. B **37**, 325 (1988).
- 46. I. F. Herbut, Phys. Rev. B **58**, 971 (1998)
- 47. J. V. Jose, L. P. Kadanoff, S. Kirkpatrick, and D. R. Nelson, Phys. Rev. B **16**, 1217 (1977).
- 48. R. Mukhopadhyay and P. B. Weichman, Phys. Rev. Lett. **76**, 2977 (1996).